Silencing of p53 and CDKN1A establishes sustainable immortalized megakaryocyte progenitor cells from human iPSCs

AUTHOR(S):

Sone, Masamitsu; Nakamura, Sou; Umeda, Sachiko; Ginya, Harumi; Oshima, Motohiko; Kanashiro, Maria Alejandra; Paul, Sudip Kumar; ... Iwama, Atsushi; Eto, Koji; Takayama, Naoya

CITATION:

Sone, Masamitsu ...[et al]. Silencing of p53 and CDKN1A establishes sustainable immortalized megakaryocyte progenitor cells from human iPSCs. Stem Cell Reports 2021, 16(12): 2861-2870

ISSUE DATE:

2021-12

URL:

http://hdl.handle.net/2433/266571

Stem Cell Reports
Report
ISSCR
OPEN ACCESS

Silencing of *p53* and *CDKN1A* establishes sustainable immortalized megakaryocyte progenitor cells from human iPSCs

Masamitsu Sone,[1,8,9] Sou Nakamura,[2,9] Sachiko Umeda,[1] Harumi Ginya,[3] Motohiko Oshima,[4] Maria Alejandra Kanashiro,[1] Sudip Kumar Paul,[1] Kanae Hashimoto,[2] Emiri Nakamura,[2] Yasuo Harada,[2] Kyoko Tsujimura,[1] Atsunori Saraya,[5] Tomoyuki Yamaguchi,[6] Naoshi Sugimoto,[2] Akira Sawaguchi,[7] Atsushi Iwama,[4] Koji Eto,[1,2,*] and Naoya Takayama[1,*]

[1]Department of Regenerative Medicine, Chiba University Graduate School of Medicine, Chiba, Japan
[2]Department of Clinical Application, Center for iPS Cell Research and Application, Kyoto University, Kyoto, Japan
[3]Megakaryon Corporation, Kyoto, Japan
[4]Division of Stem Cell and Molecular Medicine, Center for Stem Cell Biology and Regenerative Medicine, The Institute of Medical Science, The University of Tokyo, Tokyo, Japan
[5]Department of Cellular and Molecular Medicine, Graduate School of Medicine, Chiba University, Chiba, Japan
[6]Laboratory of Regenerative Medicine, Tokyo University of Pharmacy and Life Science, Tokyo, Japan
[7]Ultrastructural Cell Biology, Department of Anatomy, Faculty of Medicine, University of Miyazaki, Miyazaki, Japan
[8]Present address: Hibernation Metabolism, Physiology and Development Group, Institute of Low Temperature Science, Hokkaido University, Sapporo, Japan
[9]These authors contributed equally
*Correspondence: kojieto@cira.kyoto-u.ac.jp (K.E.), tnaoya19760517@gmail.com (N.T.)
https://doi.org/10.1016/j.stemcr.2021.11.001

SUMMARY

Platelet transfusions are critical for severe thrombocytopenia but depend on blood donors. The shortage of donors and the potential of universal HLA-null platelet products have stimulated research on the *ex vivo* differentiation of human pluripotent stem cells (hPSCs) to platelets. We recently established expandable immortalized megakaryocyte cell lines (imMKCLs) from hPSCs by transducing *MYC*, *BMI1*, and *BCL-XL* (*MBX*). imMKCLs can act as cryopreservable master cells to supply platelet concentrates. However, the proliferation rates of the imMKCLs vary with the starting hPSC clone. In this study, we reveal from the gene expression profiles of several MKCL clones that the proliferation arrest is correlated with the expression levels of specific cyclin-dependent kinase inhibitors. Silencing *CDKN1A* and *p53* with the overexpression of *MBX* was effective at stably inducing imMKCLs that generate functional platelets irrespective of the hPSC clone. Collectively, this improvement in generating imMKCLs should contribute to platelet industrialization and platelet biology.

INTRODUCTION

Platelet transfusion is a critical measure for severe thrombocytopenia to prevent or treat lung, intestinal, or intracranial hemorrhage (Ho-Tin-Noé et al., 2018). However, aging societies in many developed countries anticipate future shortages of blood products due to the imbalance of young populations donating blood and aged populations demanding transfusions. In response to this situation, we previously established human pluripotent stem cell (hPSC)-derived megakaryocyte progenitor cells by introducing doxycycline (Dox)-inducible *MYC*, *BMI1*, and *BCL-XL* (*MBX*), which we named immortalized megakaryocyte cell lines (imMKCLs) (Nakamura et al., 2014). imMKCLs show sustained proliferation over several months and subsequent maturation after Dox removal (*MBX*-off), leading to platelet generation. imMKCLs can also be stocked for several months in liquid nitrogen as a master cell stock. Furthermore, we recently succeeded in generating HLA class I-depleted induced PSC (iPSC)-derived platelets, which should contribute to the worldwide supply of universal platelet concentrates (Suzuki et al., 2020).

Platelet concentrates containing 2–3 × 10^{11} platelets are usually used in clinical settings, and nearly the equivalent number can be generated from 2–3 × 10^{9} *MBX*-off imMKCLs in 6 days (Ito et al., 2018; Nakamura et al., 2014; Takayama et al., 2008, 2010). To stably produce these concentrates, a huge number of imMKCL master cell stocks are required. For example, theoretically, the preparation of 1,000 platelet concentrates (equal to 10^{14} platelets) requires over 10^{12} imMKCLs. However, in our recent attempts, we succeeded in inducing imMKCLs, which continuously proliferate for over 60 days and 10^{12} fold, from less than 5% of hPSC clones. Such a low success rate restricts the universalization of this technology.

In this study, by comparing the global transcriptional profiles of MKCL lines, we found that two cyclin-dependent kinase inhibitors (CDKIs), *CDKN1A* and *CDKN2A*, were associated with proliferation defects after *MBX* overexpression. Knockdown of *CDKN1A* and also of *p53* efficiently increased the induction efficiency of MKCL proliferation for over 60 days and 10^{12} fold without affecting the megakaryocyte (MK) maturation for platelet generation.

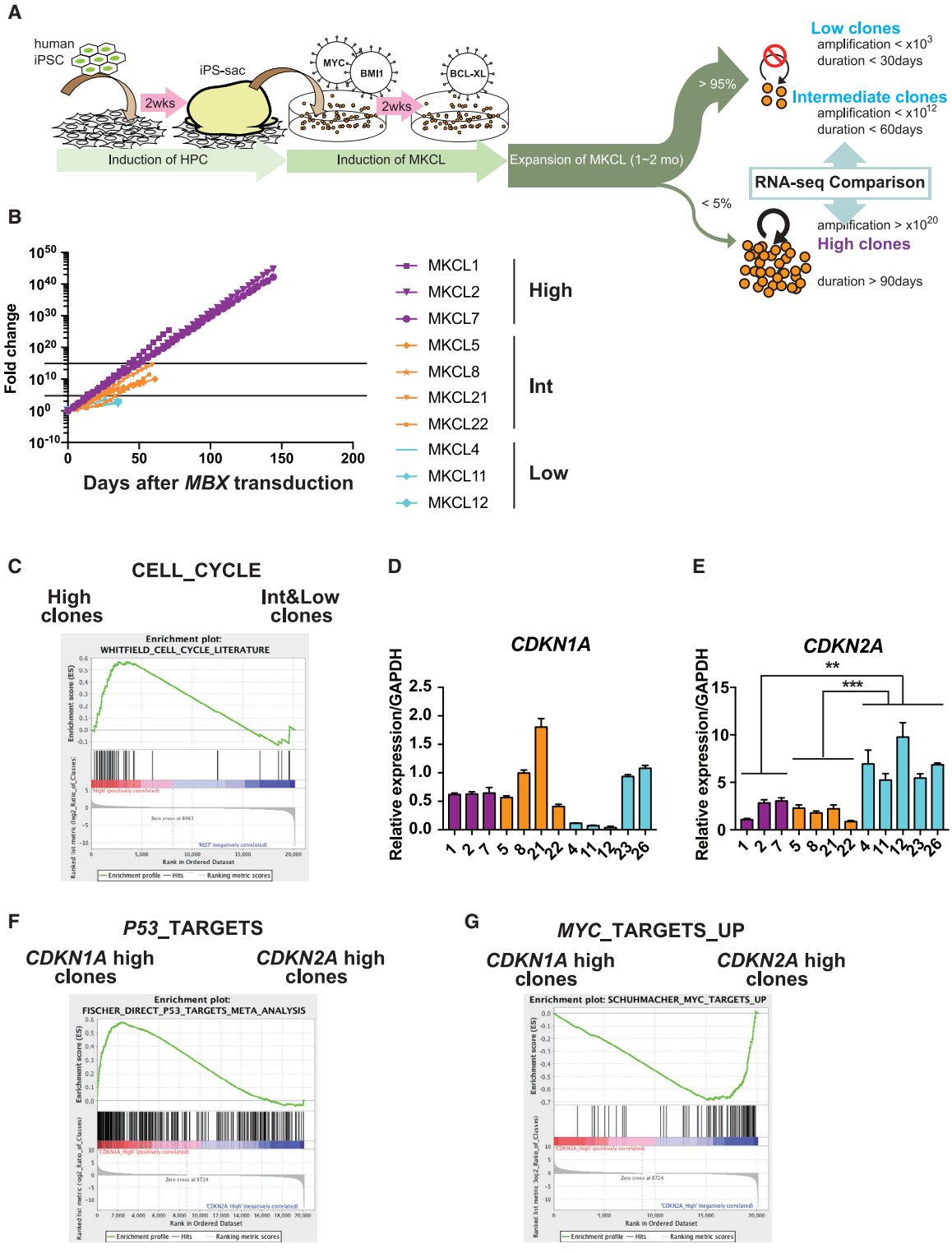

Figure 1. Heterogeneous upregulation of CDKIs in MKCL clones

(A) Scheme of MKCL induction by the standard protocol.

(B) Growth curves of ten MKCL clones.

(C) GSEA plot of the "Cell Cycle" gene set between High and Low/Int MKCL clones.

(legend continued on next page)

RESULTS

Cyclin-dependent kinase inhibitors had higher expression levels in low/intermediate proliferative MKCL clones

We classified ten MKCL samples induced by the transduction of *MBX* into hematopoietic progenitor cells (HPCs) from different human iPSC clones into three groups: clones that proliferate over 10^{20} fold and for over 90 days (High), clones that proliferate less than 10^{12} fold and for less than 60 days (Int), and clones that proliferate for less than 30 days (Low) (Figures 1A and 1B; Table S1). We regarded MKCLs that meet the criteria for High clones as immortalized lines, namely imMKCLs. To clarify the underlying mechanism that inhibits the continuous proliferation of MKCLs, we performed RNA sequencing (RNA-seq) on the three High clones (MKCL1, 2, and 7) at different time points (days 28–43 and 120–128) after the *MBX* transduction as well as on the four Int clones (MKCL5, 8, 21, and 22; days 30–55) and three Low clones (MKCL4, 11, and 12; days 33–39). We confirmed that the variation in the proliferation potential was not due to different *MBX* expression levels (Figures S1A–S1C). A gene set enrichment analysis (GSEA) showed that 186 and 1,258 gene sets were enriched (false discovery rate <25%) in the High and Int/Low groups, respectively (Table S2). Among them, we noticed that cell-cycle-, apoptosis-, and senescence-related pathways were significantly enriched (Figure 1C and Table S2). Among CDKIs that might regulate these pathways, the expression of *CDKN1A* ($p = 0.19$) and *CDKN2A* ($p = 0.29$) showed a tendency to be higher in the Int/Low group (Figures S1D and S1E), although the difference was not statistically significant. We compared the expression levels of CDKIs among the groups by qRT-PCR and found that *CDKN1A* did not show statistical differences between any combinations of groups but that when we looked at the individual clones, the four clones (MKCL8, 21, 23, 26) showing the highest *CDKN1A* expression belonged to the Int and Low groups and not the High group (Figures 1D and S1F). Moreover, all of the Low clones showed higher expression levels of *CDKN2A* than High or Int clones (Figures 1E and S1F). A comparative analysis between *CDKN1A*-high and *CDKN2A*-low clones (MKCL21, 22) and *CDKN2A*-high and *CDKN1A*-low clones (MKCL11, 12) by GSEA suggested that p53 tumor-suppressor and MYC pathways are activated in these clones, respectively (Figures 1F and 1G). However, *MYC* did not show a significant correlation with *CDKN2A* expression at the transcriptional level, which may indicate that MYC upregulates *CDKN2A* by unknown mechanisms in Low clones (Figure S1G). Surprisingly, the expression of *BMI1*, which is a well-known repressor of *CDKN2A* gene and is overexpressed under Dox control, had some positive correlation with *CDKN2A*, possibly indicating undetermined negative feedback between BMI1 and CDKN2A in some Low MKCLs (Figure S1H). In total, the high expression levels of *CDKN1A* and/or *CDKN2A* were associated with the low proliferation potentials of MKCLs and may be stimulated by the p53 and MYC pathways, respectively.

Knockdown of CDKN1A and/or p53 reactivates growth potential of low-proliferation MKCL clones

From the above data, we hypothesized that CDKIs and p53 are involved in MKCL proliferation arrest. Therefore, we treated Int/Low MKCLs with lentiviral vectors harboring short hairpin RNA (shRNA) sequences for *CDKN1A*, *CDKN2A*, and *p53* (Figure 2A). The knockdown of *CDKN1A* in MKCL21 and MKCL22, which showed high *CDKN1A* but low *CDKN2A* expression (Figures 1D and 1E), accelerated MKCL growth (Figures 2B, 2C, S2A, and S2B). Importantly, MKCL21 transduced with shCDKN1A showed stable proliferation after a freeze-thawing procedure for over 300 days and a 10^{66} fold increase in MK number (Figure S2C). We named this reactivated cell line MKCL21#. Next, we analyzed the effect of suppressing *p53* in MKCL21 and MKCL22, finding that it enhanced the proliferation of both clones (Figures 2B, 2C, S2D, and S2E). In contrast, the knockdown of *CDKN2A* or *p53* in Low clones MKCL11 and MKCL12, which showed high *CDKN2A* and low *CDKN1A* expressions, did not have any positive effect on their proliferation (Figures 2D, 2E, S2F, and S2G). These results suggest that the p53-CDKN1A axis regulates MKCL proliferation arrest in some Int clones and that the single knockdown of *p53* or *CDKN1A* at the proliferation arrest stage can rescue proliferation in these clones. In contrast, the knockdown of only *p53* or *CDKN2A* was insufficient to reactivate proliferation in Low clones, which showed high *CDKN2A* and low *CDKN1A* expressions.

Notably, the suppression of *CDKN1A* significantly upregulated *p53* (Figures S2D and S2E), suggesting that the simultaneous downregulation of CDKIs and *p53* may rescue the proliferation potential more effectively than the knockdown of only one. Based on this idea, we attempted to rescue MKCL23 and MKCL26, which showed severe proliferation arrest and highly expressed both CDKIs, by

(D and E) mRNA levels of *CDKN1A* (D) and *CDKN2A* (E) in MKCLs. Bar plots show means ± SEM from three independent experiments. $^{**}p < 0.01$; $^{***}p < 0.001$.
(F and G) GSEA plots of the "P53_Targets (F)" and "MYC_Targets (G)" gene sets between high *CDKN1A*/low *CDKN2A* clones and low *CDKN1A*/high *CDKN2A* clones.

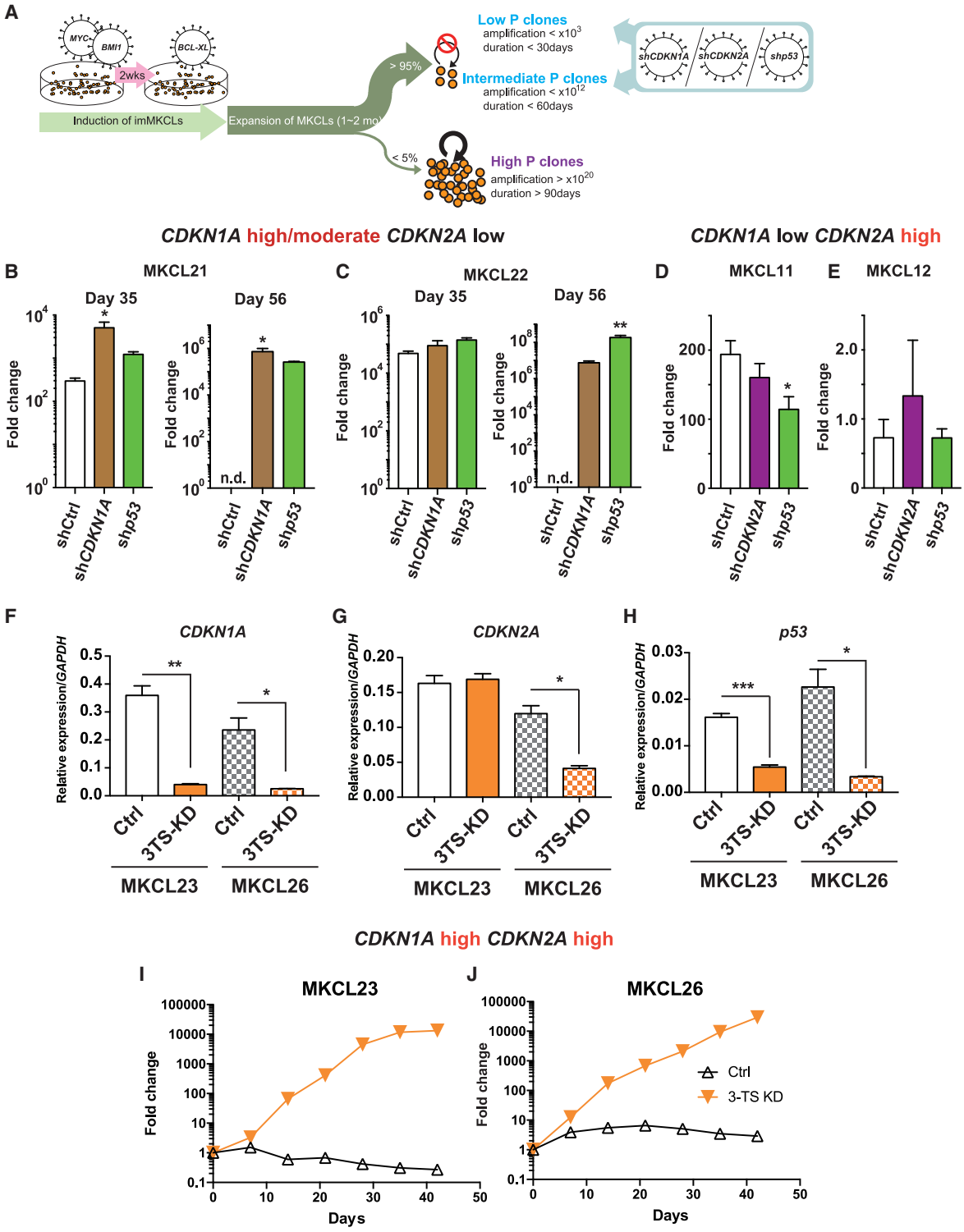

Figure 2. Knockdown of CDKIs in Int/Low MKCL clones renders re-proliferation potential at the proliferation arrest stage

(A) Scheme of the knockdown experiments at the proliferation arrest stage.

(B and C) Fold change of MKCL21 (B) and MKCL22 (C) 35 and 56 days after the shRNA transduction.

(D and E) Fold change of MKCL11 (D) and MKCL12 (E) on day 35.

(legend continued on next page)

knocking down all three tumor suppressors: *CDKN1A*, *CDKN2A*, and *p53* (hereafter designated as 3-TS). The cocktail of the three shRNAs could repress these genes by more than half except for *CDKN2A* in MKCL23 (Figures 2F–2H) and remarkably activated the proliferation of both clones (Figures 2I and 2J).

Knockdown of cyclin-dependent kinase inhibitors significantly improves the induction efficiency of immortalized MKCLs by MYC/BMI1/BCL-XL overexpression

These results motivated us to examine the growth-promoting effect of 3-TS knockdown not only on the proliferation arrest stage but also on the induction stage of imMKCLs to establish a universal protocol for most iPSC clones. To examine the optimal timing and combination of shRNAs for the transduction to induce imMKCLs, we selected three good manufacturing process (GMP)-grade human iPSC clones, YZWJ 513, 516, and 524, from which we previously failed to induce imMKCLs by *MBX* overexpression (Nakamura et al., 2014). The clones were differentiated into HPCs via the iPS-sac method for 14 days (Takayama and Eto, 2012; Takayama et al., 2008, 2010) and then transduced with Dox-inducible *MYC* and *BMI1* overexpression vectors. Two weeks after the *MYC/BMI1* transduction, we transduced *BCL-XL* (Nakamura et al., 2014) and various combinations of 3-TS shRNAs (Figure 3A).

First, we evaluated the effect of 3-TS knockdown by introducing shRNAs along with *BCL-XL* into MKCLs derived from YZWJ 524 and found that the transduced cells could proliferate continuously over 70 days, a period not achieved when transducing only *MBX* into these clones (Figure S3A).

Next, we sought the optimal combination of shRNAs by introducing all combinations into MKCLs derived from the YZWJ 513 and 516 iPSC clones and evaluated the proliferative capacity compared with no knockdown control (Ctrl). Knocking down either *CDKN1A* or *p53* but not *CDKN2A* in YZWJ 513 increased MKCL proliferation (Figures 3B and 3C). Moreover, we observed that the combined introduction of two or more shRNAs had a stronger effect on the proliferation activation than any one shRNA in MK progenitors derived from YZWJ 513 and 516. Especially, YZWJ 513 and 516 MKCLs introduced with shRNAs targeting *CDKN1A* and *p53* consistently showed higher proliferation capacity (Figures 3B and 3C) and expression of CD41$^+$ CD42b MK specific markers (Figures 3D–3G). We named these clones MKCL29 and MKCL30, respectively. To show the reproducibility of this method, we also established two new MKCLs, MKCL31 and MKCL32, by *MBX* overexpression in combination with shCDKN1A/shp53 from PB3-1 iPSCs (Figures S3B and S3C). Next, to analyze the effective timing of the *CDKN1A* and *p53* double knockdown, we transduced the shRNAs into MKCLs derived from YZWJ 513 and 516 a week after the infection of *BCL-XL* and compared the proliferation capacity with that of MKCLs transduced with the shRNAs and *BCL-XL* simultaneously (Figure 3A). Although both experiments increased the proliferation of MKCLs, the effect was stronger with the simultaneous transduction (Figures 3H and 3I). These data indicate that knocking down CDKIs and *p53* at earlier time points promotes the induction of highly proliferative MKCLs. Consistently, the expression of CDKIs was initiated from as early as the HPC stage and was significantly increased with MB (transduction of *MYC* and *BMI1* only) or *MBX* transduction in Low clones (Figures S3D–S3I). Notably, no iPSC clones examined expressed significant levels of CDKIs (Figures S3D–S3I) and showed no significant difference in their proliferation rates (Figure S3J).

Overall, these results suggest that the combinatorial transduction of shRNAs against *CDKN1A* and *p53* (with or without *CDKN2A* shRNA) at the same time as *BCL-XL* transduction improves the induction efficiency of imMKCLs from three iPSC clones from which we could not generate imMKCLs by a previous method.

Immortalized MKCLs induced with CDKN1A and p53 knockdown generate functional platelets

To examine the terminal differentiation and platelet generation capacity of the imMKCLs induced by our novel methodology, we quantified the CD42b expression of MKs and the number of CD41$^+$ CD42b$^+$ platelets in clones into which we introduced shCDKN1A (MKCL21#), shCDKN1A, and shp53 (MKCL30) or neither (MKCL21, 22, 26) along with MKCL7 as a positive control. As shown previously, MKCL7 showed higher CD42b expression and generated a higher number of CD41$^+$ CD42b$^+$ platelets in the *MBX*-off condition than in the Dox (*MBX*)-on condition (Figures 4A, 4B, and S4A–S4D) (Nakamura et al., 2014). Importantly, MKCL21# and MKCL30 expressed differentiation markers at a level similar to that of MKCL7 and produced numbers of platelets comparable with MKCL7 upon Dox withdrawal (Figures 4A, 4B, and S4A–S4D). Furthermore, the efficiencies of the platelet release in MKCL21# and MKCL30 were significantly higher than of MKCL21 and MKCL26, which were respectively derived from the same iPSC lines but by transduction with only *MBX* (Figures 4A, 4B, and

(F–H) mRNA levels of *CDKN1A* (F), *CDKN2A* (G), and *p53* (H) in MKCL23 and MKCL26 clones with shCtrl and 3TS.
(I and J) Growth curves of MKCL23 (I) and MKCL26 (J) transduced with indicated shRNAs.
All bar plots show means ± SEM from three independent experiments. *p < 0.05; **p < 0.01; ***p < 0.001.

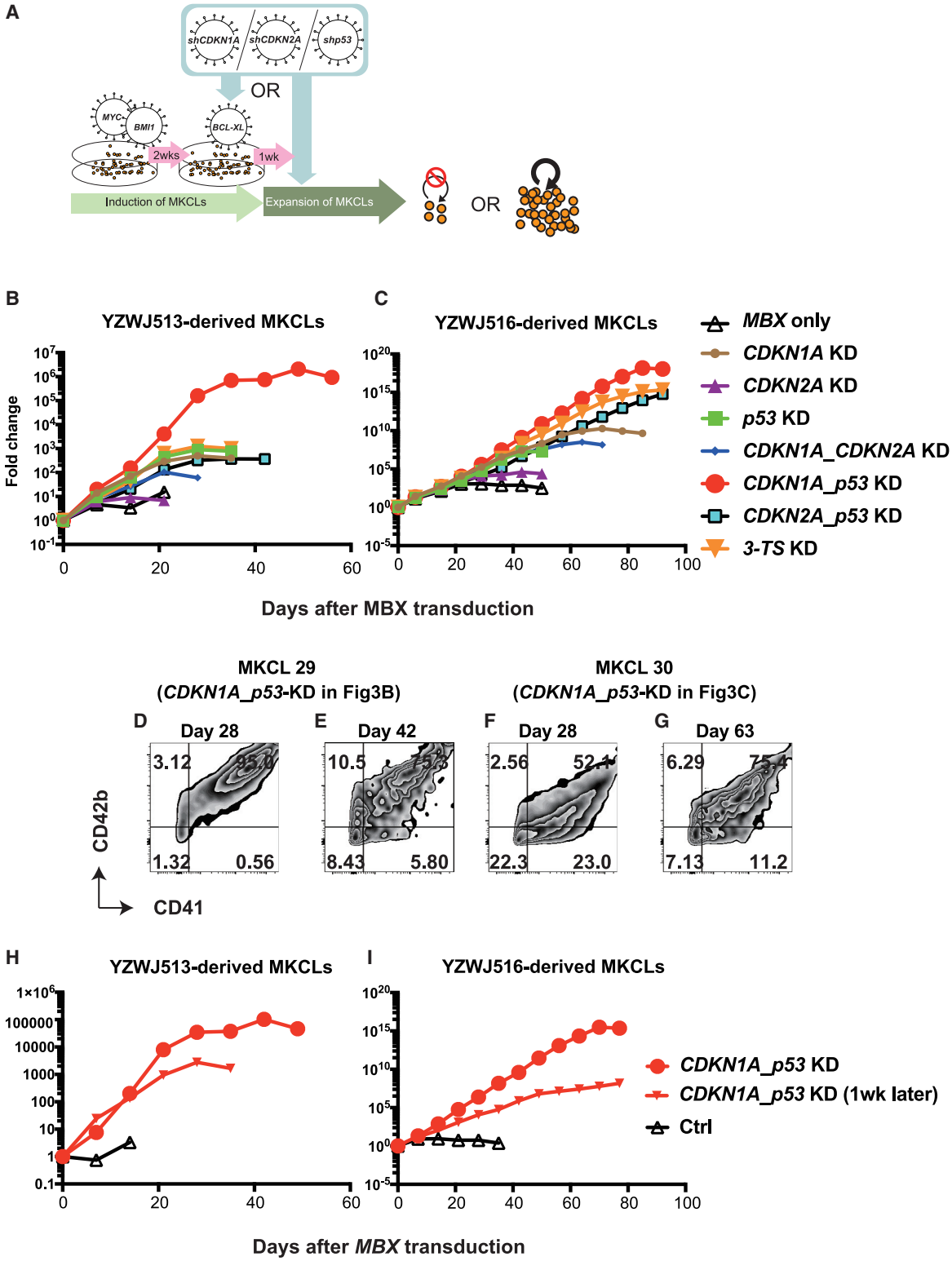

Figure 3. Knockdown of CDKIs significantly improves the induction efficiency of imMKCLs from human iPSCs by *MYC/BMI1/BCL-XL* overexpression

(A) Scheme of the induction of MKCLs by *MBX* and shRNAs.

(legend continued on next page)

S4A–S4D). Consistently, in MKCL30 we observed well-developed demarcation membrane systems resembling those in MKLC7, but observed hardly any in MKCL26 (Figures S4E–S4G). These data indicate that the continuous expression of shCDKN1A and/or shp53 does not inhibit platelet generation, but *MBX* overexpression does. We also determined the karyotypes of imMKCLs including those established using shRNAs and found that MKCL30 showed several types of chromosomal abnormalities (Figures S4H–S4J; see discussion).

Finally, we analyzed the functionality of the platelets by integrin αIIb/β3 activation (inside-out signaling) and P-selectin expression after stimulation with platelet agonists. Both integrin αIIb/β3 activation and P-selectin expression in $CD41^+$ $CD42b^+$ platelets were induced by the administration of 0.4 μM phorbol 12-myristate 13-acetate (PMA) or 100 μM ADP + 40 μM TRAP6, but not in $CD41^+$ particles generated in *MBX*-on (Figures 4C–4E). Collectively, imMKCLs, in which *CDKN1A* and *p53* were continuously suppressed, generated platelets with comparable function and yield.

DISCUSSION

The heterogeneous differentiation potential of human iPSC clones is a large obstacle for the realization of regenerative cell therapies with stable supply. We have attempted to generate imMKCLs from dozens of human iPSC clones. However, the induction efficiency of imMKCLs that continuously proliferated over 90 days was less than 5%, which motivated us to search for additional factors other than *MBX*.

To identify the underlying mechanism of the MKCL proliferation arrest, we performed RNA-seq and compared the gene expression profiles of MKCL clones with high and intermediate/low proliferation potential. A GSEA revealed that cell-cycle- and CDKN1A-p53-related pathways were significantly enriched. We found that *CDKN1A* is expressed at various levels, but that *CDKN2A* was highly expressed in Low MKCL clones and lowly expressed in High and Int clones. Knockdown experiments revealed that the proliferation arrest of MKCLs was caused by CDKN1A and its upstream factor, p53. The combinatorial knockdown of these two factors increased the proliferation potential compared with the knockdown of only one factor. This effect may be due to the repressive regulation of *p53* by CDKN1A through a negative feedback loop (Figures S2D and S2E). Another possibility is that CDKN1A and p53 may have unique targets even though they are known to share similar pathways (Löhr et al., 2003; Millau et al., 2016). Moreover, by transducing shRNAs against *CDKN1A* and *p53* simultaneously with BCL-XL, we were able to successfully establish new imMKCLs from three GMP-grade human iPSC clones, from which we had never established imMKCLs by our previous methodology.

Growing evidence has suggested that CDKN1A is not just a downstream factor of p53 but that CDKN1A complexes with p53 and targets multiple cellular processes, including autophagy, apoptosis, the epithelial-mesenchymal transition, cancer cell invasion, and cell-cycle checkpoints (Bunz et al., 1998; Kim et al., 2014; Mohapatra et al., 2012; Zhang et al., 2013). In lung cancer cells, the function of BCL2 family proteins is suppressed by the CDKN1A/p53 complex, which in turn liberates BAX to promote apoptosis through caspase activation (Kim et al., 2017). In our MKCL system, the anti-apoptotic effect of BCL-XL is essential for long-term MKCL self-replication (Nakamura et al., 2014), and the combined knockdown of *CDKN1A* and *p53* might contribute to the maintenance of BCL-XL function.

CDKN2A encodes p16INK4A and p14ARF, which regulate permanent cell-cycle arrest, i.e., senescence. MKCLs of low proliferation potential showed high *CDKN2A* expression, which we suspected caused the growth arrest (Figure 1E). However, the knockdown of *CDKN2A* alone or in combination with other CDKIs did not clearly improve the self-replication ability of MKCLs under *MBX* overexpression. These results suggest that although a higher expression of *CDKN2A* is associated with defective cell growth, the expression of *CDKN2A* itself is not the cause of proliferation arrest but a consequence of cell-cycle inhibition, which may be evoked by unspecified MYC-dependent pathways (Figure 1G).

Finally, we confirmed that functional platelets were generated from imMKCLs by continuously suppressing *CDKN1A* and *p53*. CDKN1A and p53 are critical inhibitors of tumorigenesis, which could prohibit cell types in which they are suppressed for clinical applications. However, because platelets are anucleate cells and can be irradiated before transfusion, there is no risk for cancer development. Thus, our new strategy, i.e., the overexpression of *MBX* and knockdown of *CDKN1A/p53*, is a universal methodology to induce imMKCLs and will therefore contribute to the study of platelet biogenesis and the industrialization of artificial platelet concentrates.

(B and C) Growth curves of YZWJ 513 (B) and YZWJ 516 (C) iPSC-derived MKCLs transduced with the indicated shRNAs along with BCL-XL.
(D–G) Representative flow-cytometry plots showing MKCL29 (D, day 28; E, day 42) and MKCL30 (F, day 28; G, day 63).
(H and I) Growth curves of YZWJ 513 (H) and YZWJ 516 (I) iPSC-derived MKCLs transduced with indicated shRNAs on the same day as or 1 week after *BCL-XL* overexpression. The day of *BCL-XL* transduction was set to day 0.

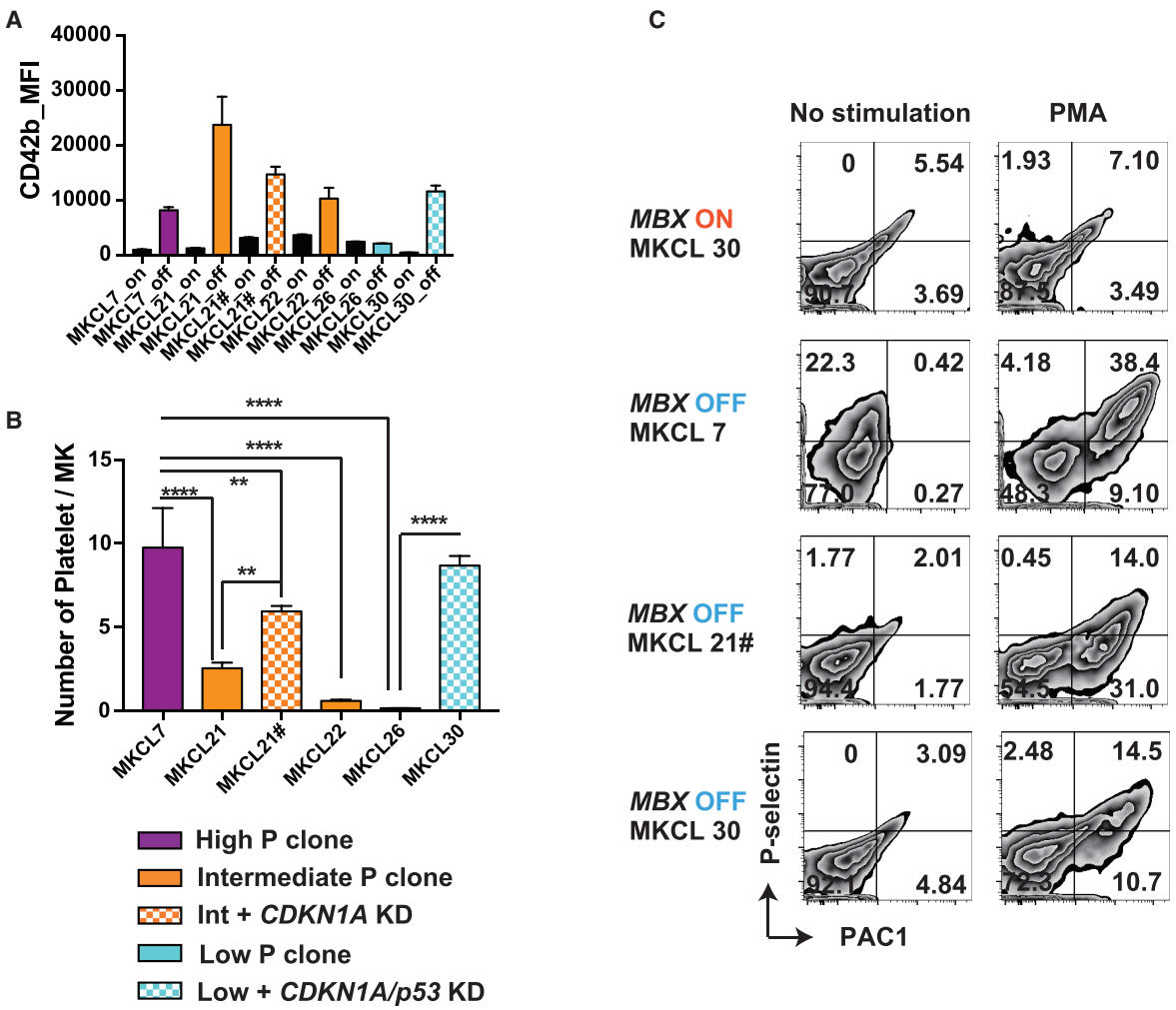

(legend on next page)

EXPERIMENTAL PROCEDURES

Cell culture and reagents

MKCL7 was induced by Dox-inducible defined factors as previously described (Nakamura et al., 2014). Other MKCL clones were established by the same method at the Department of Clinical Application, Center for iPS Cell Research and Application (CiRA), Kyoto University, and Megakaryon (Kyoto, Japan) (Table S1) and cultivated in the presence of 50 ng/mL human SCF (R&D Systems), 50 ng/mL human TPO (R&D Systems), and 100 μg/mL Dox (Clontech) (Nakamura et al., 2014). Human iPSCs were kind gifts from CiRA and Megakaryon (Table S1). All studies were performed in accordance with the Declaration of Helsinki and approved by the ethics committee in Chiba University.

The following antibodies were used for the flow-cytometric analysis: allophycocyanin (APC)-conjugated anti-CD41a (integrin αIIbβ3 complex: HIP8 clone) (Biolegend, San Diego, CA), phycoerythrin (PE)-conjugated anti-CD42b (GPIbα) (eBioscience, San Diego, CA), PE-conjugated anti-CD41a (HIP8 clone) (Biolegend), fluorescein isothiocyanate-conjugated anti-PAC-1 (BD Biosciences), and APC-conjugated anti-P-selectin (AK4 clone) (Biolegend).

Lentiviral production

Oligonucleotides of shRNA against *CDKN1A* and *LacZ* (control) were inserted into CS-CDF-Rfa-EPR lentiviral vector plasmid DNA. shCDKN2A-GFP (Nakamura et al., 2014; Voorhoeve and Agami, 2003) and shp53-GFP (Brummelkamp et al., 2002; Nakamura et al., 2014) vectors were kind gifts from Kyoto University.

The inserted oligonucleotide sequences are as follows:

shControl, CCG GTG TTG GCT TAC GGC GGT GAT TTC TCG AGA AAT CAC CGC CGT AAG CCA ACT TTT TG;
shCDKN1A, GAT CCC CAG AGG TTC CTA AGA GTG CTG GCT CGA GCC AGC ACT CTT AGG AAC CTC TTT TTT GGA AAT.

Obtained plasmid DNA was co-transfected with pMD2.G and psPAX2 (both from Addgene) into HEK293T cells using the CalPhos Mammalian Transfection Kit (Clontech). HEK293T cells were maintained in Iscove's modified Dulbecco's medium (IMDM; Gibco) supplemented with 10% fetal calf serum and penicillin/streptomycin-L-glutamine (PSG; Gibco). After the medium change with IMDM (10% fetal bovine serum, PSG, 1 mM sodium butyrate [Sigma-Aldrich, #B5887]) on the next day, lentiviruses were concentrated using the Optima L-100 XP Ultracentrifuge (Beckman Coulter; Rotor type 19, 19,000 rpm, 4.5 h, 4°C), and titrated on MOLM-13 AML cell lines.

Lentiviral transduction into MKCLs to rescue MKCL proliferation arrest

INT/LOW MKCLs induced by Dox-inducible factors (*MYC/BMI1/BCL-XL*; *MBX* overexpression) at the proliferation arrest stage were transduced with lentiviral vectors harboring shRNA for LacZ (shControl), *CDKN1A*, *CDKN2A*, and/or *p53* at a multiplicity of infection of 1–3.

Induction of MKCLs by combinatorial transduction of *MBX* and CDKI shRNAs

MKCL clones were induced as previously described. In brief, HPCs differentiated from human iPSCs (Takayama et al., 2008, 2010) were transduced with Dox-inducible lentiviral vectors harboring MYC and BMI1 to induce MK-lineage cells (Nakamura et al., 2014). Two weeks after the *MYC* and *BMI1* transduction, MK cells were transduced with Dox-inducible lentiviral vectors harboring *BCL-XL*. Lentiviral vectors harboring shRNA for *CDKN1A*, *CDKN2A*, and/or *p53* were transduced simultaneously with the *BCL-XL* transduction or 2 weeks later (Figure 3A).

Statistical analysis

All data are presented as means ± SEM. The statistical significance of observed differences was determined by one-way ANOVA followed by Tukey's multiple comparison test and two-tailed Student's t tests for pairwise comparisons. Values of $p < 0.05$ were considered significant.

Data and code availability

Raw and normalized microarray data have been deposited in the Bioinformation and DDBJ Center under accession numbers SAMD00238010 to SAMD00238021.

SUPPLEMENTAL INFORMATION

Supplemental information can be found online at https://doi.org/10.1016/j.stemcr.2021.11.001.

AUTHOR CONTRIBUTIONS

N.T. designed the experiments. The induction of MKCLs was performed by M.S., S.N., S.U., M.A.K., S.K.P., and K.H. Bioinformatics analysis of the RNA-seq was performed by N.T., M.S., and H.G. with assistance from A. Saraya, M.O., and A.I. Inducible lentiviral vectors were constructed by S.N. and T.Y. Lentiviral production was performed by T.Y., K.T., and S.N. Platelet functional analysis was performed by E.N. and Y.H. Transmission electron microscopy of MKs was done by A. Sawaguchi. M.S., S.N., N.S., K.E., and N.T. wrote the paper. The study was supervised by K.E. and N.T.

Figure 4. imMKCLs induced with continuous knockdown of CDKN1A and p53 generate functional platelets

(A) Mean fluorescence intensity (MFI) of CD42b in MKCLs.

(B) Average number of platelets generated from a single MK 6 days after Dox withdrawal.

(C–E) Flow-cytometric analysis of platelets generated by MKCLs with or without agonists. (C) Representative flow-cytometry plots showing PAC1 and P-selectin expression in the presence or absence of 0.4 μM PMA. Percentage of P-selectin-positive (D) and PAC1-positive (E) platelets in the $CD41^+$ population in the presence or absence of 0.4 μM PMA or 100 μM ADP + 40 μM TRAP6.

All bar plots show means ± SEM from three independent experiments. *$p < 0.05$; **$p < 0.01$; ***$p < 0.001$; ****$p < 0.0001$; n.s., not significant.

DECLARATION OF INTERESTS

M.S., S.N., K.E., and N.T. have applied for patents related to this manuscript. K.E. is a founder of Megakaryon and a member of its scientific advisory board without salary. This work was supported in part by grants from Megakaryon to N.T. The interests of K.E. were reviewed and are managed by Kyoto University in accordance with its conflict-of-interest policies. Y.H. is an employee of Otsuka Pharmaceuticals.

ACKNOWLEDGMENTS

We acknowledge the staff at Megakaryon for providing human iPSCs and MKCL clones, and Dr. Peter Karagiannis for critical reading of the manuscript. This work was supported in part by the Mochida Memorial Foundation for Medical and Pharmaceutical Research (M.S.), SENSHIN Medical Research Foundation (M.S.), Terumo Life Science Foundation (K.E.), Practical Applications of Regenerative Medicine (JP17bk0104039, K.E.), Projects for Technological Development (JP19bm0404037h0002, N.S. and K.E.), Core Center for iPS Cell Research (JP17bm0104001, S.N., N.S., and K.E.), The Program for Technological Innovation of Regenerative Medicine, Research Center Network for Realization of Regenerative Medicine (20bm0704051h0001, S.N., N.S., and K.E.) from the Japan Agency for Medical Research and Development (AMED), The Program for Technological Innovation of Regenerative Medicine, Research Center Network for Realization of Regenerative Medicine (21bm0404072h0001, S.N. and N.T., and 21bm0704051h0002, K.E.) from AMED, and by a grant-in-aid for scientific research (18H04164, S.N. and K.E.; 21H05047, S.N., N.S., and K.E.; 18K18365, S.N.; 20K08705, N.T.) from the Japan Society for the Promotion of Science. N.T. obtained a research budget from Megakaryon.

Received: October 1, 2020
Revised: November 1, 2021
Accepted: November 1, 2021
Published: December 2, 2021

REFERENCES

Brummelkamp, T.R., Bernards, R., and Agami, R. (2002). A system for stable expression of short interfering RNAs in mammalian cells. Science *296*, 550–553.

Bunz, F., Dutriaux, A., Lengauer, C., Waldman, T., Zhou, S., Brown, J.P., Sedivy, J.M., Kinzler, K.W., and Vogelstein, B. (1998). Requirement for p53 and p21 to sustain G2 arrest after DNA damage. Science *282*, 1497–1501.

Ho-Tin-Noé, B., Boulaftali, Y., and Camerer, E. (2018). Platelets and vascular integrity: how platelets prevent bleeding in inflammation. Blood *131*, 277–288.

Ito, Y., Nakamura, S., Sugimoto, N., Shigemori, T., Kato, Y., Ohno, M., Sakuma, S., Ito, K., Kumon, H., Hirose, H., et al. (2018). Turbulence activates platelet biogenesis to enable clinical scale ex vivo production. Cell *174*, 636–648.e18.

Kim, E.M., Jung, C.-H., Kim, J., Hwang, S.-G., Park, J.K., and Um, H.-D. (2017). The p53/p21 complex regulates cancer cell invasion and apoptosis by targeting Bcl-2 family proteins. Cancer Res. *77*, 3092–3100.

Kim, J., Bae, S., An, S., Park, J.K., Kim, E.M., Hwang, S., Kim, W., and Um, H. (2014). Cooperative actions of p21 WAF 1 and p53 induce slug protein degradation and suppress cell invasion. EMBO Rep. *15*, 1062–1068.

Löhr, K., Möritz, C., Contente, A., and Dobbelstein, M. (2003). p21/CDKN1A mediates negative regulation of transcription by p53. J. Biol. Chem. *278*, 32507–32516.

Millau, J.-F., Wijchers, P., and Gaudreau, L. (2016). High-resolution 4C reveals rapid p53-dependent chromatin reorganization of the CDKN1A locus in response to stress. PLoS One *11*, e0163885.

Mohapatra, P., Preet, R., Das, D., Satapathy, S.R., Choudhuri, T., Wyatt, M.D., and Kundu, C.N. (2012). Quinacrine-mediated autophagy and apoptosis in colon cancer cells is through a p53- and p21-dependent mechanism. Oncol. Res. *20*, 81–91.

Nakamura, S., Takayama, N., Hirata, S., Seo, H., Endo, H., Ochi, K., Fujita, K., Koike, T., Harimoto, K., Dohda, T., et al. (2014). Expandable megakaryocyte cell lines enable clinically applicable generation of platelets from human induced pluripotent stem cells. Cell Stem Cell *14*, 535–548.

Suzuki, D., Flahou, C., Yoshikawa, N., Stirblyte, I., Hayashi, Y., Sawaguchi, A., Akasaka, M., Nakamura, S., Higashi, N., Xu, H., et al. (2020). iPSC-derived platelets depleted of HLA class I are inert to anti-HLA class I and natural killer cell immunity. Stem Cell Reports *14*, 49–59.

Takayama, N., and Eto, K. (2012). In vitro generation of megakaryocytes and platelets from human embryonic stem cells and induced pluripotent stem cells. Methods Mol. Biol. *788*, 205–217.

Takayama, N., Nishikii, H., Usui, J., Tsukui, H., Sawaguchi, A., Hiroyama, T., Eto, K., and Nakauchi, H. (2008). Generation of functional platelets from human embryonic stem cells in vitro via ES-sacs, VEGF-promoted structures that concentrate hematopoietic progenitors. Blood *111*, 5298–5306.

Takayama, N., Nishimura, S., Nakamura, S., Shimizu, T., Ohnishi, R., Endo, H., Yamaguchi, T., Otsu, M., Nishimura, K., Nakanishi, M., et al. (2010). Transient activation of c-MYC expression is critical for efficient platelet generation from human induced pluripotent stem cells. J. Exp. Med. *207*, 2817–2830.

Voorhoeve, P.M., and Agami, R. (2003). The tumor-suppressive functions of the human INK4A locus. Cancer Cell *4*, 311–319.

Zhang, Y., Yan, W., Jung, Y.S., and Chen, X. (2013). PUMA cooperates with p21 to regulate mammary epithelial morphogenesis and epithelial-to-mesenchymal transition. PLoS One *8*, e66464.